Bulletin of the Geological Survey of Japan, vol. 42 (4), p. 199-220, 1991

Geochemistry of sediments from the flank province of Costa Rica Rift in the Panama Basin

Hodaka KAWAHATA[***], Saburo AOKI[***], Steven D. SCOTT[**] and Toshio ISHIZUKA[†]

Kawahata, H., Aoki, S., Scott, S.D. and Ishizuka, T. (1991) Geochemistry of sediments from the flank province of Costa Rica Rift in the Panama Basin. *Bull. Geol. Surv. Japan*, vol. 42 (4), p. 199-220, 6 fig., 8 tab.

Abstract: ODP Sites 677 and 678 are located in the equatorial high productivity zone of the Panama Basin. Sediments from both sites are composed mainly of biogenic materials. Their sand and silt size fractions contain much biogenic carbonate and silica as well as detrital material. Clay-size fractions are clay minerals and biogenic fragments. It is suggested that the aluminous smectites, the most dominant clay mineral, originated on land were transported, and deposited at Sites 677 and 678 without change of their original chemical compositions whereas Fe-rich smectites from these sites are of hydrothermal origin.

The contents of Mn, Cu and Zn in the sediment cores are relatively low due to dilution by abundant carbonate. However, a negative Ce anomaly and a good correlation between these metals/Al and REEs/Al ratios indicate that these metals are partly incooperated into hydrothermal products. Especially Mn, Cu, and Zn extracted by hydroxylamine hydrochloride-acetic acid solution would be atrributed to hydrothermal precipitates. The accumulation rates of hydrothermal Mn, Cu and Zn were 4.7-6.2 mg/cm^{2}10^{3}yr, 29-78 μg/cm^{2}10^{3}yr and 121-366 μg/cm^{2}10^{3}yr from 6.2 Ma to 2.2 Ma, and decreased to 0.6-1.9 mg/cm^{2}10^{3}yr, 11-48 μg/cm^{2}10^{3}yr and 64-94 μg/cm^{2}10^{3}yr from 2.2 Ma to the present, respectively. Hydrothermal Mn accumulation rate of Hole 677 A is comparable to those near the spreading center of East Pacific Rise. Such high and constant accumulation rates of heavy metals from 6.2 Ma to 2.2 Ma in Hole 677 A are probably due to the contribution of flank hydrothermal activity.

1. Introduction

Seawater-basalt interaction at elevated temperature produces an acidic, reduced and heavy metal-rich solution (Edmond *et al.*, 1979 ; Von Damm *et al.*, 1985). When it is venting into cold, alkalic, oxygenated seawater, a variety of hydrothermal precipitates form within the vent or in the plume (e.g., Bolger *et al.*, 1978 ; Edmond *et al.*, 1979 ; McConachy and Scott, 1987 ; Trocine and Trefry, 1988). Hydrothermal precipitates in the plume may settle immediately to the seafloor or be transported varying distances from the vent field.

Basement basalts of Hole 504 B which originated at the Costa Rica Rift, reacted with seawater at temperatures above 300°C near the spreading center and subsequently moved about 200 km southward during the last 6.2 million years (Anderson *et al.*, 1982 ; Alt *et al.*, 1986 ;

* Marine Geology Department
** Department of Geology, University of Toronto
*** Toyo University
† Ocean Research Institute, University of Tokyo

Keywords: hydrothermal activity, hydrothermal origin, hydrothermal precipitates, smectite, accumulation rate, high productivity zone, biogenic material

Kawahata *et al.*, 1987). Because the young basement is covered with thick sediments which act as a thermal blanket, the present temperature of the sheeted dike zone is 165°C at 1562.3 m subbottom depth (Leg 111 Shipboard Scientific Party, 1987). Sites 677 and 678 are located several kilometers from Hole 504 B and were drilled to the basement during ODP Leg 111. These two holes provide sedimentary records for tracing continuous hydrothermal inputs to the sediments during the last 6 million years because there has been little or no sedimentary hiatus in the area (Leg 111 Shipboard Scientific Party, 1988).

In this paper, we report (1) the relative abundances of various components of sediments, (2) chemical compositions of bulk sediments and separated fine size fractions, (3) the characteristics of the smectites, and (4) the concentrations of extractable Mn, Cu and Zn. Our objectives are (1) to discuss the relation between bulk geochemistry and constituent materials in the sediments, (2) to determine the origin of the smectites, (3) to estimate metal accumulation rates and (4) to compare sediments on the flank of the Costa Rica Rift from those of the East Pacific Rise.

2. Materials and methods

2.1 Lithology and downhole properties of Sites 677 and 678

Two holes were cored at Site 677 (1°12.14′, 83°44.22′W) in a water depth of 3,461 m. Hole 677 A was cored to 309.4 m subbottom depth (Fig. 2 A). Hole 677 B was offset from Hole 677 A by 10 m to 30 m, reaching 97.1 m subbottom depth. Site 678 was drilled at 1°13.01′N, 83°43.39′W in a water depth of 3435 m (Fig. 1). The Site 677 is located at a lower heat flow zone (166 mW/m^2) while 678 is at a higher heat flow zone (250 mW/m^2) (Langseth *et al.*, 1988 ; ODP Leg 111 Shipboard Scientific Party, 1988).

Three major sedimentary units and a basal basalt unit are recognized in Hole 677A (ODP Leg 111 Shipboard Scientific Party, 1988). Lithologic Unit I consists of alternating clayey biogenic calcareous siliceous oozes and clayey biogenic siliceous calcareous oozes, ranging in age from early Pliocene to late Pleistocene (0–153.8 m subbottom depth). Unit II is

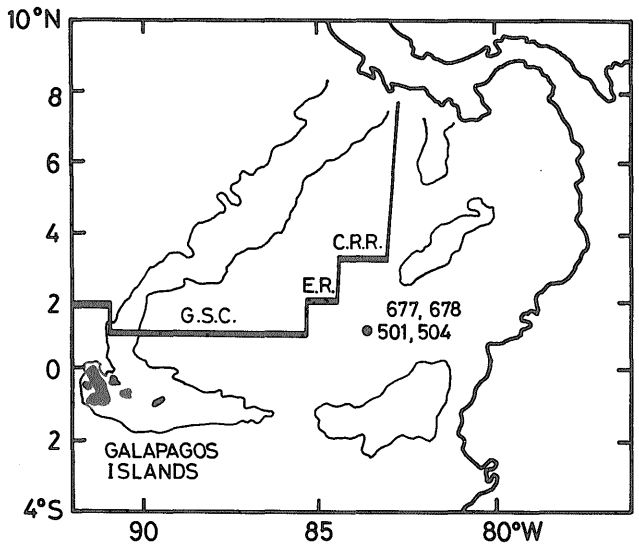

Fig. 1 Locations of ODP Sites 501, 504, 677 and 678 in the Panama Basin of the Costa Rica Rift. (G.S.C.=Galapagos Spreading Center ; E.R.=Ecuador Rift ; C.R.R.=Costa Rica Rift)

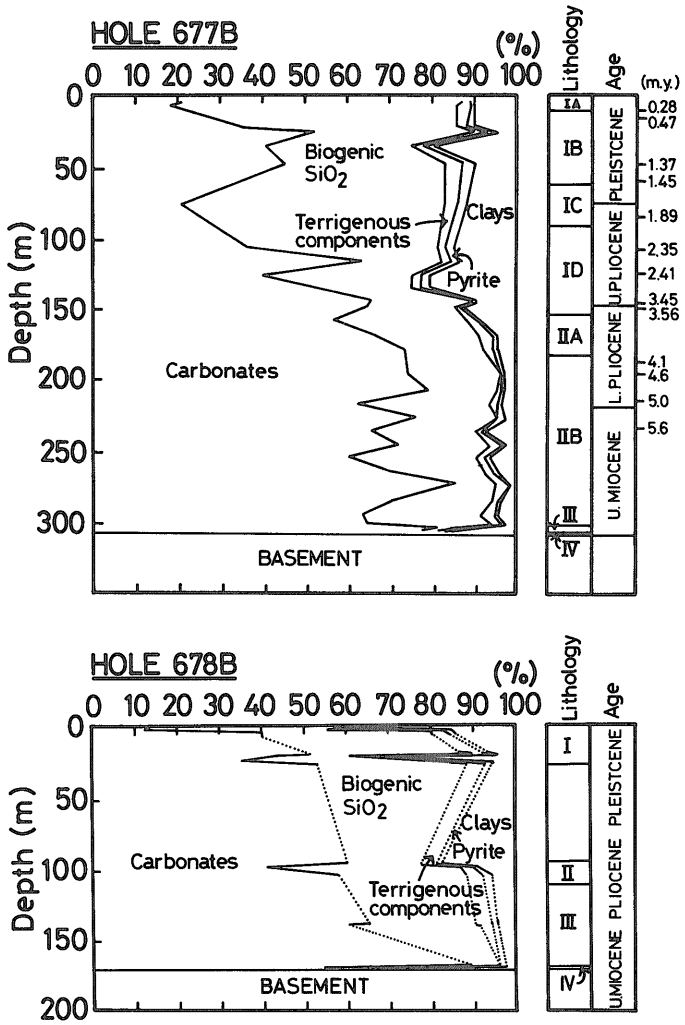

Fig. 2 Composition of the sediments of Holes 677 A (A) and 678 B (B) based upon smear slide observations.

composed of siliceous nannofossil ooze and chalk, and ranges in age from late Miocene to early Pliocene (153.8–303.3 m). Unit III consists of cherty limestone and nannofossil chalk and is late Miocene in age (303.3–308.5 m). Unit IV consists of iron oxide and smectite rich sediments intermixed with glassy basement basalts of late Miocene age (308.5–309.4 m).

The sedimentation rate, established in Hole 677 A micro fossils, averages 48m/m.y. and shows little variation down to 5.95 Ma (Leg 111 Shipboard Scientific Party, 1988). Porosity ranges from 91.1% at the seafloor surface to 53.1% at the base of Hole 677 A. Corresponding bulk densities are 1.20g/cm^3 to 1.84 g/cm^3 and, in general, decrease as a function of subbottom depth (Leg 111 Shipboard Scientific Party, 1988). Downhole temperature was measured only in the upper 100 m. Linear extraporation yields a basement temperature on the order of 60–70°C.

Hole 678 B was drilled to 170.1 m subbottom depth (Fig. 2 B). Three sedimentary units and one basaltic unit are recognized. Unit I is composed of clayey calcareous siliceous ooze (0.0–27.7 m). Unit II consists of clayey diatom

nannofossil chalk (95.5–111.8 m). Unit III is composed of limestone (111.8–169.8 m), and Unit IV consists of basalt fragments and conglomerate (169.8–170.1 m).

2. 2 Analytical procedures

Bulk chemistry

The analyses of major and minor elements (Si, Ti, Al, Fe, Mn, Mg, Ca, Na, K, P, Zr, Y and Nb) of bulk sediments were performed by X-ray fluorescence spectrometry (XRF). Instrument precision is within 5% for these elements. Heavy metals (Co, Cr, Cu, Ni, and Zn), Sr and Rb were analysed by atomic absorption spectrometry (AA) after digestion with HF, HNO_3 and H_2SO_4 (Kawahata and Furuta, 1985). Precision estimated from replicate analyses is within 5%. Standards were JB-1 a, JB-2, JB-3, JA-1, JA-2, JG-1 and JG-2 from Geological Survey of Japan. Neutron activation analysis (NAA) was done at the Slowpoke Reactor Facility, University of Toronto. The concentration of 18 elements (Fe, Na, Cs, Ba, Sc, Hf, Ta, Th, U, La, Ce, Nd, Sm, Eu, Tb, Tm, Yb, and Lu) were determined. Sealing 200 mg aliquots of sample and standards in polyethylene bags, irradiating and counting with gamma ray spectrometers after 7 days and 50 days. The precision of NAA analysis was not always better than that obtained by XRF or AA. Only the best results are quoted when more than one analytical method was used.

Chemistry of fine size fractions

The <2 μm and size fractions separated by centrifuge were digested with HF, HNO_3 and H_2SO_4 and analysed by ion coupled plasma (ICP). Precision estimated from replicate analyses of the samples is within 2%.

Identification of clay minerals

Ultrasonically agitated and dispersed material of <0.2 μm and 0.2–2 μm size fractions, separated by centrifuge were examined. The clay minerals were identified by X-ray diffraction patterns and by scanning electron images.

Extraction analysis

Pelagic sediment samples were dissolved in hydroxylamine hydrochloride-acetic acid solutions for 4 hours in order to separate trace elements incorporated into the sediment by ferro-manganese oxide and/or hydroxide, by carbonate minerals and by adsorption onto mineral surfaces. This procedure is similar to that of Chester and Hughes (1967).

3. Results

3. 1 Smear slides

Hole 677 A

Results of the examination of smear slides for Hole 677 A are shown in Table 1 and Fig. 2 A. The sand and silt size fractions (>4-μm) are mostly biogenic carbonate and silica. Within the calcareous fraction, nannofossils are the dominant constituents. They always exceed the proportions of foraminifers and of unspecified carbonate which may be foraminifer fragments based upon their size and the distribution. Relatively low percentages of <30 % carbonate are only found in Subunits IA and IC. Relatively high percentages of >60% are found, below 160 m subbottom depth, in Units II, III and IV.

Within the siliceous fossil fraction, the percentage of diatoms commonly exceeds that of radiolarians, and each of these fossil groups forms a significantly larger portion than do sponge spicules and silicoflagellates, which are rarely >10%. Sponge spicules are generally more common than silicoflagellates. In Lithologic Unit I the percentages of siliceous fossils mainly range between 30 and 60%, and in Lithologic UNit II are often <30% in Lithologic Unit II. The percentage of clay is almost always >10% in Lithologic Unit I, ranging from 2 to 9% in Unit II, and is around 15% in Unit III.

Hole 677 B

Smear slide data for Hole 677 B sediments are presented in Table 1. The mineralogies and their contents are almost the same as those in Unit I of Hole 677 A.

Hole 678 B

Smear slide data for Hole 678B sediments are in Table 1 and Fig. 2 B. Nannofossils are the dominant constituent within the calcareous fraction, always exceeding the proportions of foraminifers and unspecified carbonate. Fairly low percentages (<30%) of carbonate are

Table 1 Smear slide abundances in sediments from Holes 677 A, 677 B and 678 B.

C-S Interval			1	2	3	4	5	6	7	8	9	10	11	12	13	14
677 A																
1	3	145–150	4.5	2	14	5	31	25	10	0	0	0	2	0	1	10
2	1	80–90	7.0	3	10	5	30	36	2	0	0	2	1	0	1	10
3	4	120–125	21.4	3	27	5	15	25	10	1	1	1	0	0	2	10
4	1	55–74	25.8	4	38	10	20	12	5	1	0	0	0	3	2	5
5	1	51–69	35.3	1	27	12	19	13	3	0	1	1	0	1	2	20
6	3	120–125	48.4	4	24	17	12	18	6	2	2	0	0	2	3	10
9	3	120–125	76.9	3	12	5	39	20	2	2	2	0	0	1	2	12
12	4	120–125	106.9	3	23	10	28	12	3	2	2	0	0	0	2	15
13	4	145–150	116.7	5	48	10	7	7	5	0	1	1	0	0	2	14
14	4	145–150	126.2	5	27	7	15	10	4	7	1	0	0	1	2	21
15	4	120–125	135.4	5	31	15	15	4	5	0	0	1	0	1	2	21
16	4	145–150	145.2	5	47	13	9	8	7	0	0	0	0	0	1	10
17	3	145–150	148.7	5	49	10	10	7	3	1	0	0	0	1	1	13
18	3	120–125	158.0	5	43	8	17	11	3	1	0	1	0	1	1	9
19	4	145–150	169.5	5	46	15	9	12	3	1	0	1	1	1	1	5
20	4	145–150	179.2	5	53	15	6	6	7	0	1	0	0	1	1	5
22	3	120–125	196.6	2	62	10	13	5	3	1	0	0	0	0	1	3
23	4	145–150	208.1	7	62	10	5	6	4	1	0	0	1	0	1	3
24	4	145–150	217.7	3	54	5	16	9	5	1	0	0	1	1	1	4
25	4	120–125	227.1	1	70	5	7	7	4	1	0	0	0	0	2	3
26	4	145–150	237.1	1	61	3	19	3	3	0	0	0	1	0	1	8
27	4	145–150	246.8	4	63	5	10	3	7	1	0	1	1	1	1	3
28	3	120–125	254.6	1	56	3	20	4	5	1	0	1	1	0	1	7
29	3	145–150	264.5	5	60	4	10	5	7	1	0	1	1	0	1	5
30	3	145–150	274.2	4	76	5	3	3	3	1	1	1	0	1	0	2
31	4	120–125	285.0	2	65	3	10	10	3	1	0	0	1	0	1	4
32	4	145–150	294.9	1	59	3	12	10	5	1	0	2	1	0	1	5
33	2	145–150	301.6	2	57	5	16	7	5	2	0	1	0	1	1	3
33	4	145–150	304.6	2	74	5	0	2	1	0	0	0	0	0	1	15
33	5	123–140	305.9	2	70	5	0	4	0	0	0	1	0	0	1	17
677 B																
1	1	95–100	1.0	2	16	10	17	26	3	1	0	2	1	1	1	20
1	2	145–150	3.0	3	38	7	18	15	4	0	0	2	1	1	1	10
2	3	145–150	12.1	2	42	10	13	7	5	0	1	2	0	1	1	16
3	1	145–150	18.6	1	43	5	12	10	3	1	0	2	1	1	1	20
3	4	145–150	23.1	3	43	5	5	13	4	1	2	2	1	1	2	18
4	1	145–150	28.1	3	21	7	25	15	5	1	1	1	1	1	2	17
4	3	145–150	31.1	3	25	7	17	11	6	1	0	1	1	2	3	23
5	1	145–150	37.6	2	37	10	15	10	6	1	0	2	1	1	1	14
5	3	145–150	40.6	1	24	7	19	18	5	3	1	3	1	1	1	16
6	4	120–125	51.3	3	34	6	18	12	5	1	0	3	2	1	1	14
8	4	145–150	70.6	2	41	4	15	11	4	1	1	2	0	0	1	18
9	4	145–150	80.1	2	10	7	22	13	15	1	2	0	1	2	1	24
10	4	145–150	89.6	3	50	3	19	6	8	1	1	2	2	0	2	3

Table 1 (Continued)

C-S Interval			1	2	3	4	5	6	7	8	9	10	11	12	13	14
678 B																
1	1	45–50	0.5	3	5	5	29	21	4	0	0	2	1	1	1	28
1	1	145–150	1.5	2	5	5	12	25	5	1	0	2	0	1	2	40
1	2	145–150	3.0	4	29	7	25	10	5	0	0	2	0	1	2	15
2	1	45–50	18.7	7	40	5	12	18	3	1	0	2	0	4	1	7
2	1	145–150	19.7	3	35	4	17	25	4	1	1	2	0	2	1	5
2	2	145–150	21.2	3	34	4	6	9	4	0	0	2	1	1	2	34
2	4	145–150	24.2	4	25	5	25	11	4	0	0	2	1	1	2	20
2	5	145–150	25.7	8	41	4	21	9	5	0	0	2	1	2	1	6
3	1	145–150	97.0	3	53	4	10	3	4	0	0	2	1	1	1	18
3	3	120–125	99.7	3	33	4	25	15	5	2	0	1	1	1	1	9
3	6	145–150	104.5	1	54	3	18	7	4	1	1	2	0	1	2	6
4	2	55–67	138.0	5	55	5	13	8	4	0	0	1	1	2	1	5
4	3	95–107	138.9	0	58	2	17	9	5	0	0	2	0	1	1	5
4	4	145–150	139.9	2	60	3	15	7	3	0	0	1	2	1	1	5
4	CC	3–15	168.9	2	85	2	3	3	1	0	0	0	0	0	1	3
4	CC	30–42	169.2	0	52	2	2	2	1	0	0	0	0	3	1	37

Note :

1 : Subbottom depth
2 : Foraminifers
3 : Calcareous nannofossils
4 : Unspecified carbonate
5 : Diatoms
6 : Radiolarians
7 : Sponge spicules
8 : Silicoflagellates
9 : Quartz
10 : Feldspar
11 : Volcanic glass
12 : Accessory minerals
13 : Pyrite
14 : Clay minerals

Table 2 Relative clay mineral abundances of 0.2–2 μm and <0.2 μm fractions from Holes 677 A and 678 B.

Hole	677A							678B			
Core	3	9	12	14	16	28	33	1	2	2	3
Section	4	3	4	4	4	3	4	1	1	5	3
Interval	114	116	113	139	138	114	100	50	39	139	115
(cm)	120	122	120	146	145	120	106	56	45	145	121
0.2–2 μm fraction											
smectite	88	78	80	—	81	72	100	79	74	65	50
chlorite	6	8	20	—	11	—	—	6	13	26	—
illite	—	10	—	—	5	14	—	7	13	—	—
kaolinite	6	4	—	—	3	14	—	8	—	9	50
<0.2 μm fraction											
smectite	88	67	—	—	82	77	100	84	80	81	—
chlorite	4	26	—	—	10	8	—	—	6	—	—
illite	3	7	—	—	4	8	—	—	9	—	—
kaolinite	5	—	—	—	4	7	—	16	5	19	—

found only in surface samples.

The percentages of siliceous fossils mainly range between 19% and 54%. Within the siliceous fossil fraction, diatoms and radiolarians are commonly the dominant components in Lithologic Unit I and II. The percentages of siliceous fossils are only <10% in Lithologic Unit III. The percentage of clay ranges between

Table 3 Chemical compositions of smectites and chlorite from Holes 677 A and 678 B and other fields.

Hole	677A	677A	677A	677A	677A	678B	678B	678B	678B	678B	678B	678B
Core	9	9	9	9	9	2	1	2	2	2	2	1
Section	3	3	3	3	3	1	1	1	1	1	1	1
Interval	116	116	116	116	116	39	50	39	39	39	39	50
(cm)	122	122	122	122	122	45	56	45	45	45	45	56
	Al-rich smectite	Al-rich smectite	Al-rich smectite	Al-rich smectite	Al-rich smectite	Al-rich smectite	Al-rich smectite	Fe-rich smectite	Fe-rich smectite	Fe-rich smectite	Fe-rich smectite	Fe-rich smectite
CHEMISTRY												
SiO_2	57.99	60.87	64.59	66.22	64.59	52.28	48.28	57.06	56.17	55.15	57.06	55.15
Al_2O_3	17.31	16.61	13.32	12.93	13.32	23.37	25.04	12.37	14.02	15.30	12.37	15.30
TiO_2	—	—	—	—	—	—	—	—	—	—	—	—
MgO	5.99	5.52	8.83	8.64	8.83	4.97	3.39	7.65	5.35	7.15	7.65	7.15
CaO	3.94	4.83	2.95	2.26	2.95	2.68	4.25	3.43	4.16	2.71	3.43	2.71
Fe_2O_3*	9.33	9.86	6.92	7.37	6.92	9.49	7.99	17.52	18.21	16.60	17.52	16.60
K_2O	2.55	2.28	2.16	1.30	2.16	0.94	8.16	0.92	0.78	0.62	0.92	0.62
Na_2O	2.85	0.00	1.20	1.24	1.20	6.23	2.86	1.02	1.27	2.44	1.02	2.44
TOTAL	99.96	99.97	99.97	99.96	99.97	99.96	99.97	99.97	99.96	99.97	99.97	99.97
SITE FORM												
SI	3.651	3.780	3.959	4.024	3.959	3.314	3.171	3.639	3.595	3.518	3.639	3.518
AL	1.285	1.216	0.962	0.926	0.962	1.746	1.939	0.930	1.057	1.150	0.930	1.150
TI	—	—	—	—	—	—	—	—	—	—	—	—
MG	0.562	0.511	0.807	0.783	0.807	0.469	0.332	0.727	0.510	0.679	0.727	0.679
CA	0.265	0.321	0.194	0.147	0.194	0.182	0.299	0.234	0.285	0.185	0.234	0.185
FE (3)	0.442	0.460	0.319	0.336	0.319	0.452	0.395	0.841	0.876	0.796	0.841	0.796
K	0.205	0.180	0.168	0.101	0.168	0.076	0.683	0.074	0.063	0.050	0.074	0.050
Na	0.348	0.000	0.143	0.147	0.143	0.766	0.363	0.127	0.158	0.302	0.127	0.302
	6.758	6.468	6.552	6.464	6.552	7.005	7.182	6.572	6.544	6.680	6.572	6.680

Table 3 (Continued)

Hole	678B	678B	678B	677A	677A	677A	678B	SP15At	SP15Ct
Core	1	1	1	3	9	9	1		
Section	1	1	1	4	3	3	1		
Interval	50	50	50	114	116	116	50		
(cm)	56	56	56	120	122	122	56		
	Fe-rich smectite	Fe-rich smectite	Fe-rich smectite	Mg-rich smectite	Chlorite	Chlorite	Chlorite	Al-rich smectite	Fe-rich smectite
CHEMISTRY									
SiO_2	55.97	55.15	55.97	48.84	40.93	39.04	39.04	65.00	63.56
Al_2O_3	13.14	15.30	13.14	13.65	16.25	13.00	13.00	18.94	9.01
TiO_2	—	—	—	—	—	—	—	1.55	0.98
MgO	4.92	7.15	4.92	8.67	20.71	20.18	20.18	4.75	6.85
CaO	5.35	2.71	5.35	10.55	1.95	2.65	2.65	0.30	0.38
Fe_2O_3*	17.46	16.60	17.46	13.49	15.92	17.28	17.28	6.22	14.87
K_2O	3.13	0.62	3.13	2.33	0.11	0.54	0.45	0.45	0.72
Na_2O	0.00	2.44	0.00	2.43	4.10	7.28	7.28	2.79	3.62
TOTAL	99.97	99.97	99.97	99.96	99.97	99.97	99.97	100.00	100.00
SITE FORM									
SI	3.622	3.518	3.622	3.253	2.718	2.669	2.669	3.900	3.980
AL	1.002	1.150	1.002	1.072	1.272	1.047	1.047	1.340	0.660
TI	—	—	—	—	—	—	—	0.070	0.050
MG	0.475	0.679	0.475	0.860	2.050	2.055	2.055	0.430	0.640
CA	0.371	0.185	0.371	0.752	0.139	0.194	0.194	0.020	0.030
FE (3)	0.850	0.796	0.850	0.676	0.795	0.889	0.889	0.280	0.700
K	0.258	0.050	0.258	0.198	0.009	0.047	0.470	0.030	0.060
Na	0.000	0.302	0.000	0.314	0.528	0.965	0.965	0.320	0.430
	6.578	6.680	6.578	7.125	7.511	7.866	8.289	6.390	6.550

3% and 40% through the hole.

3. 2 Clay size fractions

Clay minerals and fragments of biogenic carbonate and silica are the dominant phases in the <2 μm fraction from Holes 677 A and 678 B. The relative abundances of the four major clay minerals in the <0.2 μm and 0.2–2 μm fractions are presented in Table 2. Smectites dominate both fractions through Holes 677 A and 678 B with relative abundances averaging about 83 % in Hole 677 A and about 67% in Hole 678 B. Chlorite, kaolinite and illite are minor clay minerals in Holes 677 A and 678 B. Their average concentrations in the <0.2 μm and 0.2–2 μm fractions are about 8%, 5%, 4% in Hole 677 A and about 11%, 17%, 5% in Hole 678 B, respectively. Smectites are more enriched in finer fractions (<0.2 μm) whereas chlorite, kaolinite and illite are more depleted. These results are consistent with those obtained from coarse fraction and clay mineral distributions of surface sediments from the Panama Basin (Kowsmann, 1973 ; Moore *et al.*, 1973 ; Heath *et al.*, 1974).

3. 3 Chemical compositions of smectites and chlorite

Chemical compositions of aluminous, magnesium-rich, and iron-rich smectites and chlorite are given in Table 3 together with previous analyses of separated deep-sea clays (Aoki *et al.*, 1974 ; Aoki *et al.*, 1979). Slight contamination by fine biogenic calcareous fragments (<0.1 μm) may have lead to higher Ca values. Approximate structural formulae of the smectite phases are calculated on the basis of 10 (O) and 2 (OH) (Tables 3 and 4).

3. 4 Chemical composition of sediments

Major element geochemistry of bulk sediments

The silica content of sediments from Holes 677 A and 678 B ranges from 27% at the seafloor surface to 51% at about 200 m subbottom depth and decreases to about 20% at the base of the hole. The Si content-depth profile is controlled by the content of biogenic silica and carbonate, although relatively small amounts of clay minerals and land-derived quartz and feldspar contribute some silica (Tables 1, 5 and Figs. 2 and 3). In spite of the small distance of Holes 677 A and 678 B, there are different silica contents in Lithologic Subunits IA and IB (0–60 m subbottom depth), indicating that there is considerable lateral variation in the these subunits.

The contents of TiO_2 and Fe_2O_3 (total iron) are constant from the seafloor surface to about 110 m, decrease to about 200 m, and are constant to the bottom of the hole. MnO and MgO present similar profile except for a small increase in the upper 50 m. Al_2O_3, Na_2O and K_2O show small decreases from surface to about 110 m, large decreases down to about 200 m and constant values to the bottom of the hole.

Aluminum as well as titanum are not presented in biogenic calcareous and siliceous materials and are the least mobile element involved in any alteration or diagenetic processes. In order to eliminate the effect of variability of biogenic carbonate and silica, major elements of the sediments have been normalized relative to aluminum (Fig. 4). The profile for Ti/Al shows a gradual increase through the hole. Si/Al, Ca*/Al (noncarbonate), Ca**/Al (carbonate), P/Al and Si/Al are rather constant from the surface to 160 m

Table 4 Atomic proportions and site occupancy of smectites.

	LEG 111 Al-rich smectite	LEG 111 Fe-rich smectite	LEG 111 Mg-rich smectite	S-Pacif. Fe-rich smectite *1	DOMES Fe-rich smectite *2	N-1 non-tronite *3	Bauer smectite *4
Tetrahedral layer							
Si	3.69	3.58	3.25	3.98	3.59	3.64	3.73
Al	0.31	0.42	0.75	0.02	0.41	0.01	0.21
Fe	—	—	—	—	—	0.35	0.06
	4.00	4.00	4.00	4.00	4.00	4.00	4.00
Octahedral layer							
Al	0.96	0.63	0.32	0.64	0.91	—	—
Fe*5	0.39	0.83	0.68	0.70	0.55	1.76	1.54
Mg	0.61	0.54	0.86	0.64	0.61	0.27	0.50
	1.96	2.00	1.86	1.98	2.07	2.03	2.04
Interlayer							
Ca	0.23	0.27	0.86	0.03	0.08	0.06	0.04
Mg	—	0.07	—	—	—	—	0.15
Na	0.27	0.15	0.31	0.43	0.42	0.24	0.09
K	0.23	0.14	0.20	0.06	0.23	0.20	0.18
	0.73	0.63	1.31	0.52	0.73	0.50	0.46

*1 Aoki *et al.* (1978)
*2 Hein *et al.* (1979)
*3 Corliss *et al.* (1978)
*4 Dymond and Eklund (1978)
*5 Assumed all iron as ferric iron

Table 5 Chemical compositions of sediments from Sites 677 and 678

Hole	677A							678B			
Core	1	6	12	18	23	27	31	1	2	2	3
Section	3	6	4	3	4	4	4	1	1	5	3
Interval (cm)	148	123	123	123	148	148	123	48	48	148	123
Depth (m)	4.5	48.4	106.9	158.0	208.1	246.8	285.0	0.5	18.7	25.7	99.7
SiO_2 (%)	50.6	31.5	39.8	27.2	14.0	22.8	19.7	26.5	29.0	30.8	44.6
TiO_2	0.27	0.26	0.27	0.18	0.04	0.04	0.05	0.20	0.20	0.19	0.14
Al_2O_3	9.89	6.83	6.96	5.04	1.06	0.77	1.13	5.36	5.77	4.84	3.70
Fe_2O_3*	3.18	3.08	3.75	2.36	0.69	0.60	0.82	3.56	2.48	2.20	1.80
MnO	0.22	0.30	0.32	0.25	0.16	0.12	0.13	0.29	0.43	0.43	0.19
MgO	1.65	1.85	2.23	2.05	0.64	0.51	0.63	2.03	0.98	0.94	0.91
CaO	12.9	27.0	20.6	31.4	45.3	41.0	42.8	29.8	31.5	30.9	23.5
Na_2O	2.55	1.25	1.60	0.79	0.00	0.10	0.00	0.95	0.89	0.80	1.13
K_2O	2.24	0.47	1.03	0.28	0.01	0.04	0.03	0.25	0.40	0.23	0.69
P_2O_5	0.10	0.13	0.16	0.19	0.14	0.12	0.20	0.12	0.15	0.12	0.16
LOI	16.2	27.0	23.2	29.4	38.0	33.5	34.3	31.0	28.2	28.5	22.8
TOTAL	99.8	99.7	99.9	99.1	100.0	99.6	99.8	100.1	100.0	100.0	99.6
Co (ppm)	11	13	25	9	3	2	8	22	15	15	22
Cr	62	76	70	22	15	8	6	42	27	28	16
Cu	110	82	108	115	46	43	50	101	86	81	110
Ni	154	151	198	112	68	52	54	215	106	158	126
Zn	249	214	234	172	100	92	79	251	189	209	216
Li	39	30	33	17	12	5	2	27	24	18	4
Nb	3	2	1	2	0	0	1	1	—	—	1
Zr	67	52	54	41	14	4	14	18	—	—	34
Y	18	20	24	20	9	6	12	6	—	—	19
Sr	477	810	718	928	1067	710	1013	480	—	—	772
Rb	53	22	24	18	5	2	5	11	—	—	14
S (%)	0.80	0.51	0.24	0.50	0.28	0.28	0.28	0.18	0.26	0.37	0.62
CaCO (%)	21.19	45.43	36.58	56.06	79.06	72.17	70.4	12.58	52.2	52.74	40.27

TOC (%)	0.58	0.73	0.41	0.3	0.13	0.01	—	5.13	0.49	0.61	0.5
CaO in $CaCO_3$ (%)	11.87	25.45	20.49	31.40	44.29	40.43	39.44	7.05	29.24	29.54	22.56
Non-carbonaceous CaO (%)	1.03	1.55	0.11	0.00	1.01	0.57	3.36	22.75	2.26	1.36	0.94
Ba (ppm)	3182	2156	4179	3094	1844	1770	2243	2838	2126	2252	3441
Cs	1.4	0.7	0.8	0.6	0.1	0.1	0.1	0.5	0.7	0.5	0.4
U	6.0	5.4	5.1	3.2	1.8	2.5	2.4	6.5	5.0	5.8	3.9
Th	5.0	1.9	1.8	1.5	0.3	0.2	0.3	1.4	1.9	1.2	1.0
Sc	10.2	10.9	12.5	8.3	2.1	1.9	2.5	9.2	8.2	7.9	6.9
Hf	1.6	1.2	1.2	0.8	0.2	0.2	0.3	1.0	1.0	0.8	0.6
Ta	0.3	0.2	0.1	0.1	0.0	0.0	0.2	0.1	0.2	0.1	0.1
REE											
La (ppm)	13.6	12.0	12.5	10.0	3.2	3.8	4.2	9.1	7.7	7.8	8.4
Ce	22.8	18.2	18.7	12.8	4.1	3.4	5.0	15.2	14.9	9.5	9.9
Nd	4.2	5.0	16.9	11.0	4.6	3.0	3.8	—	10.5	—	11.4
Sm	2.3	2.4	2.4	1.8	0.6	0.6	0.7	2.0	1.5	1.7	1.5
Eu	0.5	0.6	0.6	0.4	0.2	0.1	0.2	0.5	0.4	0.4	0.3
Tb	0.4	0.4	0.4	0.3	0.1	0.1	0.1	0.3	0.2	0.3	0.2
Yb	1.5	1.7	1.9	1.6	0.7	0.7	0.8	1.4	1.0	1.2	1.4
Lu	0.1	0.3	0.2	0.2	0.1	0.2	0.1	0.3	0.1	0.3	0.1
Chondrite normalized value											
La	43.2	38.1	39.6	31.6	10.3	12.2	13.4	28.9	24.5	24.6	26.6
Ce	28.1	22.4	23.0	15.8	5.1	4.2	6.1	18.7	18.3	11.6	12.2
Nd	7.1	8.4	28.3	18.4	7.7	5.1	6.4	—	17.5	—	19.1
Sm	12.2	12.7	12.3	9.3	2.9	3.1	3.5	10.3	8.0	8.9	7.7
Eu	6.9	7.8	8.8	6.2	2.5	1.9	2.4	6.5	5.6	6.1	4.8
Tb	8.8	8.1	7.2	6.2	2.5	3.0	3.0	5.7	4.9	5.8	4.4
Lu	4.3	10.5	5.8	6.4	2.0	5.4	3.0	10.7	1.7	8.1	4.3

*Total iron

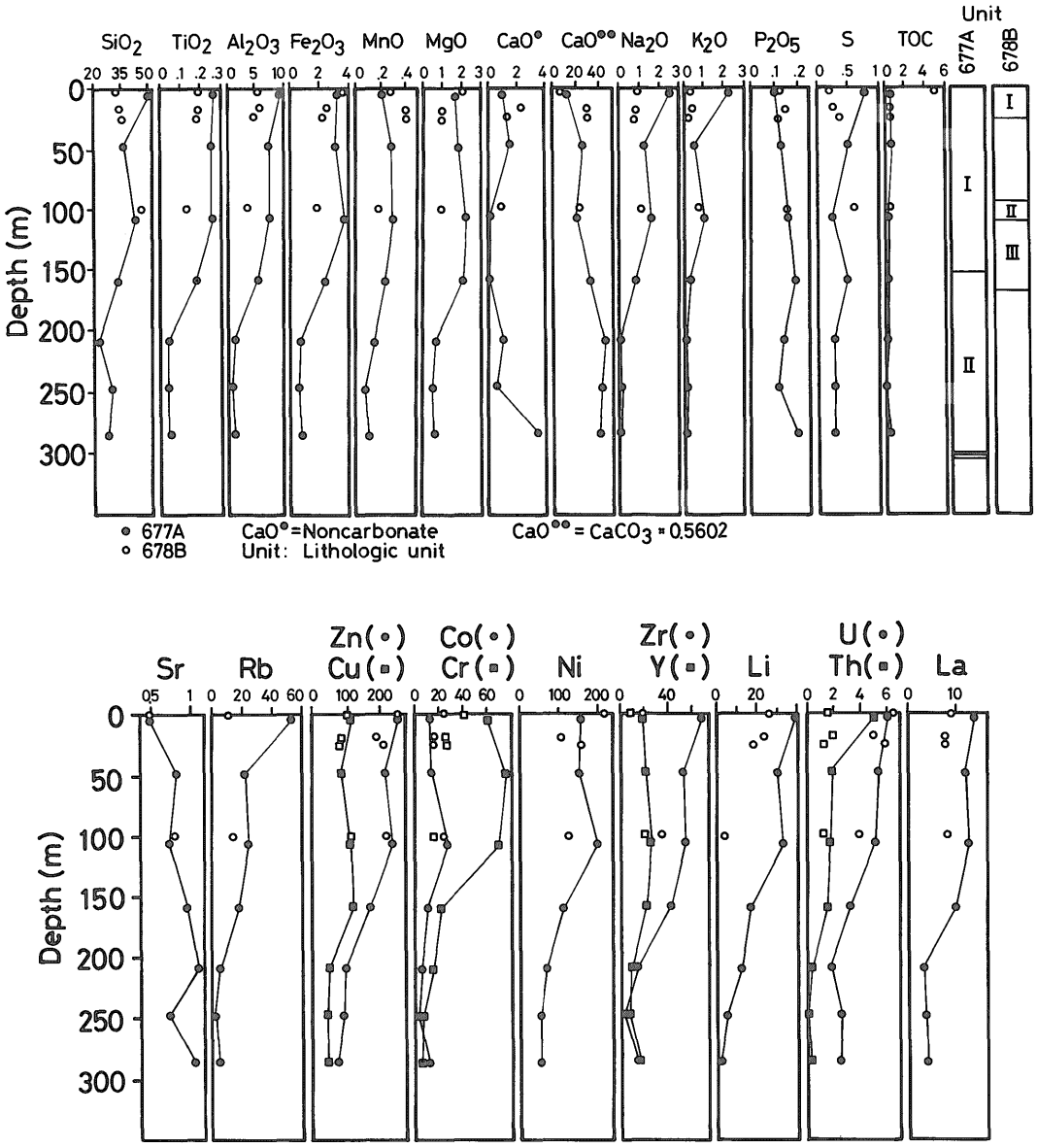

Fig. 3 Depth profiles for concentrations of major, minor and trace elements in deep-sea sediments from Holes 677 A and 678 B.

subbottom depth and increase to the bottom of the hole. Fe/Al and Mg/Al gradual increase as a function of depth. Conversely Na/Al and K/Al decrease with depth.

Aluminum-normalized profiles versus subbottom depth indicate that low contents of Si, Ti, Al, Fe, Mn, Mg, Na, K and S below 200 m subbottom depth are due to the high content of biogenic $CaCO_3$, which constitutes more than 50% of the total sediments, and that Ti, Fe, and Mg correlate rather with Al than with Ca from biogenic carbonate.

Minor and trace element geochemistry of bulk sediments

The concentrations of heavy metals (Co, Cr, Cu, Ni and Zn), and rare earth elements (REEs : La, Ce, Nd, Sm, Eu, Tb, Tm, Yb, and Lu), Li, Nb, Zr, Rb, Cs, U, Th, Sc, and Hf are

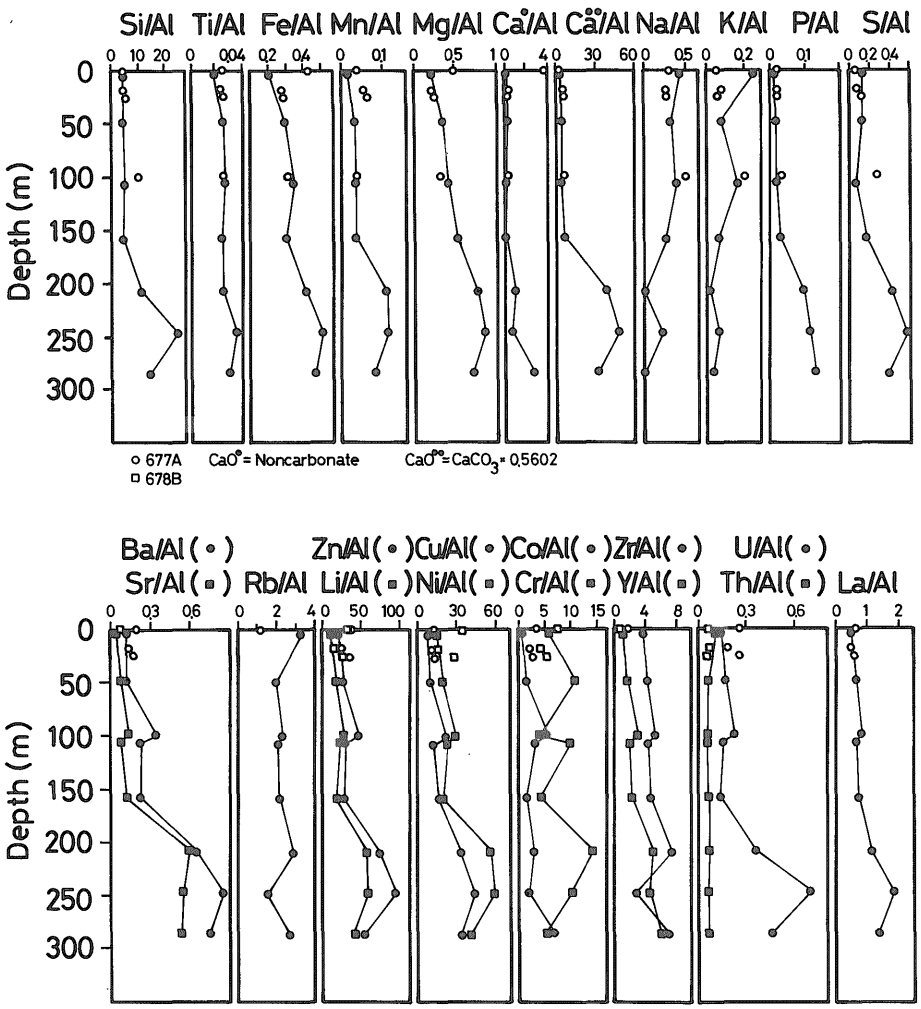

Fig. 4 Aluminium normalized sediment chemistry versus subbottom depth in Holes 677 A and 678 B.

relatively constant or decrease slightly from the seafloor surface to about 110 m subbottom depth and decrease further to the bottom of the hole (Fig. 3). These profiles are controlled by the content of biogenic carbonate and silica in the same manner as for the major elements.

The Sr/Al ratio correlates with the CaO^{**}/Al ratio, implying that Sr is contained mainly in biogenic calcium carbonate. The other alkaline earth, Ba correlates with La/Al as well as with CaO^{**}/Al. Ba is a large-ion lithophile (LIL) element and may behave like other LILs such as Cs, REEs, U and Th.

Cu/Al, Zn/Al, Ni/Al, Co/Al and Li/Al have the profiles similar to that of Mn/Al. The values for Cr/Al, Zr/Zl and Y/Al gradually increase with depth.

Total sulfur content ranges from 0.18 w.t.% to 0.80 w.t.%, averaging about 0.4 w.t.%. S/Al ratio is relatively constant from surface to about 160 m subbottom depth and then increases to the bottom of the hole.

REE elements of bulk sediments

In spite of systematic changes in the REE contents with subbottom depth (Figs. 3, 4 and 5), the sediments from Hole 677 A all have similar REE patterns : (1) there is a Ce anomaly, and (2) LREE are relatively enriched.

Table 6 Chemical compositions of <2μm size fractions of the sediments from Holes 677A and 678B.

Hole	677A				678B
Core	1	6	19	27	1
Section	3	3	4	4	1
Interval (cm)	148	123	148	148	48
Depth	4.5	48.4	169.5	246.8	0.5
Al_2O_3(%)	6.97	3.98	2.71	1.31	3.02
TiO_2	0.20	0.10	0.10	0.01	0.05
Fe_2O_3	3.49	1.45	1.09	0.22	0.94
MnO	0.30	0.38	0.18	0.03	0.20
MgO	2.45	1.37	2.08	0.23	2.13
CaO	8.01	15.95	27.27	6.35	15.76
Na_2O	3.85	3.52	11.63	0.91	13.61
Co (ppm)	18	12	6	—	5
Cr	48	25	18	—	15
Cu	209	105	311	138	81
Ni	394	214	238	88	169
Zn	400	298	139	599	102

REEs are more enriched in the upper part of the hole (from surface to 200 m subbottom depth), where the biogenic carbonate and silica content is low. This suggests that REEs are contained within non-biogenic fractions.

Major and trace elements of <2 μm size fractions

Chemical compositions of fine fractions (<2 μm) of sediments from Hole 677 A are shown in Table 6. Heavy metals such as Cu, Ni and Zn are more enriched in the fine fraction than in bulk sediments.

3. 5 Extracted heavy metals with hydroxylamine hydrochloride

Mn, Cu and Zn extracted with hydroxylamine hydrochloride-acetic acid average 0.10 w.t.%, 18ppm, and 53 ppm, respectively (Table 7). The ratios of extracted Mn, Cu, and Zn to their total contents in bulk sediments are 0.52, 0.21 and 0.3 respectively.

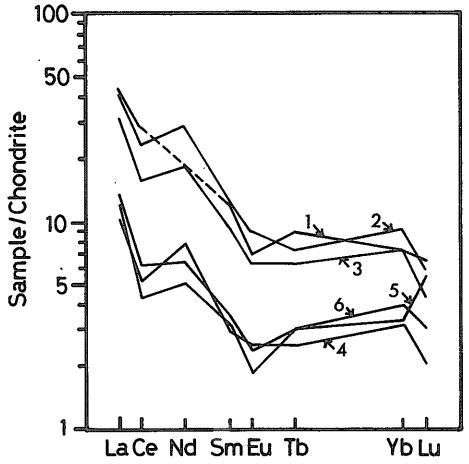

Fig. 5 Chondrite normalized rare-earth element patterns for deep-sea sediments from Hole 677 A. (1 : Core1-Section 3 145-150 cm, 2 : 12-4, 120-125 cm, 3 : 18-3, 120-125 cm, 4 : 23-4, 145-150 cm, 5 : 27-4, 145-150 cm, 6 : 31-4, 120-125 cm)

4. Discussion

4. 1 Mineralogy and geochemistry of sediments from Sites 677 and 678

Bulk sediments

The chemistry of the bulk sediments is contorolled by the constituent minerals and authigenic materials which can be divided into 7 groups : (1) detrital material (quartz, feldspar and amphibole), (2) land-derived clay minerals (illite, kaolinite and smectite), (3) original biogenic materials (carbonate, silicate and organic matter), (4) primary inorganic components (hydrothermal precipitates and ferro-

Table 7 Mn, Cu and Zn extracted with hydroxylamine hydrochloride-acetic acid from sediment of Hole 677A.

Core	1	6	12	18	23	31
Section	3	6	4	3	4	4
Intetval (cm)	148	123	123	123	148	123
Depth (m)	4.5	48.4	106.9	158.0	208.1	285.0
Mn (%)	0.054	0.108	0.134	0.127	0.070	0.057
Cu (ppm)	45	6	12	19	7	4
Zn (ppm)	60	53	99	64	35	15

manganese nodules), (5) secondary inorganic components (authigenic clay minerals, carbonate formed during diagenesis and framboidal pyrite), (6) adsorbed components (trace metals and organic materials), and (7) extraterrestrial material (tectite). Based on observations of smear slides, biogenic carbonate and silica are the most important components in sediments from Sites 677 and 678. Diagenetic reaction occurs only in lower-most part of the holes where the transformation from biogenic carbonate to limestone is found just above basement (Leg 111 Shipboard Scientific Party, 1988). However, the chemistry of the pore water is explained mainly by a simple diffusion-advection model, indicating that sedimentary particles generally preserve original chemical compositions.

CaO is contained within biogenic carbonate and inorganic minerals. Because the Panama Basin is located in the equatorial zone of biological high productivity, the amount of biogenic CaO is about 10 to 40 times greater than that of inorganic CaO. Sulfur occurs mainly as framboidal pyrite, which is common through the holes. The pyrite was probably formed during decomposition of organic matter near the surface of the sediments and was buried. This hypothesis is consistent with the observed large decrease of organic carbon content with depth (Leg 111 Shipboard Scientific Party, 1988) and the large reduction of sulfate in pore water from the uppermost 100 m of sediments at Site 504 (Mottl *et al.*, 1983). The good correlation between S/Al and Ca^{**}/Al also suggests that the formation of framboidal pyrite was favored by an abundant organic matter during rapid deposition of biogenic carbonate.

Ti/Al, Fe/Al, Mn/Al and Mg/Al gradually increase as a function of depth whereas Ca^{**}/Al is relatively constant from the surface to 160m subbottom depth and increases below 200 m. This suggests that Ti, Fe, Mn and Mg are mainly incorporated within detrital materials and/or clay minerals rather than in $CaCO_3$ and is supported by the low concentrations (several ppm) of Fe and heavy metals in foraminifera (Boyle, 1981).

The characteristics of REE patterns of bulk sediments from Hole 677 A are (1) a negative Ce anomaly and (2) REE contained mainly by non-biogenic materials. Previous studies have demonstrated that Ce in metalliferous sediments is commonly depleted relative to its abundance in chondritic meteorites (Dymond *et al.*, 1973). On the other hand, REEs in hydrogenous ferromanganese nodules generally exhibit an enrichment in Ce (Goldberg *et al.*, 1963 ; Piper, 1974). These observations indicate that the REE elements in the sediments from Hole 677 A are not related to hydrogenous Fe-Mn components.

Relation between bulk sediments and fine size fraction (<2 μm)

Ti/Al, Fe/Al and Mg/Al ratios of fine size fractions are 0.016, 0.23, and 0.52, respectively, and are similar to those of the bulk sediments. Smectite is the most important mineral in the fine fraction (Table 2). Fe/Al and Mg/Al ratios of aluminous, Fe-rich and Mg-rich smectites are, on average, 0.30 and 0.47, 0.79 and 0.58, 0.63 and 0.80, respectively, which indicates that the Fe/Al and Mg/Al ratios are controlled by aluminous smectite.

Cu/Al, Zn/Al and Mn/Al ratios are larger in the fine size fraction than in the bulk sediments. It is likely that oxides and/or hydrox-

ides of Cu, Zn and Mn account for these elevated contents of bulk sediments because common on-land smectites have low heavy metal contents. A negative Ce anomaly and a good correlation between these metals/Al and REEs/Al indicate that these metals are in part incooperated into hydrothermal products (e.g., oxides, hydroxides, Fe-rich smectites).

4. 2 Origin of smectites from Sites 677 and 678

Three genetic types of smectites occur in Sites 677 and 678. Their possible origins are (1) terrigenous: derived from continents and later dispersed by bottom waters, (2) authigenic : formed in an ash layer during early diagenesis, and (3) hydrothermal : after a reaction between hydrothermal solution and seawater.

The average chemical composition of aluminous smectite from Holes 677A and 678B is 59.3% SiO_2, 17.4% Al_2O_3, 6.6% MgO, 3.4% CaO, 8.3% Fe_2O_3* (total iron), 2.8% K_2O, and 2.2% Na_2O. The calculated formula is $Si_{3.69}Al_{1.27}Mg_{0.61}Ca_{0.23}Fe_{0.39}K_{0.23}Na_{0.27}$. The aluminous smectites from SP15At are similar to the common type formed on land. Although the chemical composition of authigenic aluminous smectite derived from andestic glass in an ash layer would be expected to be similar to that of on-land type, ash layers are not common around Sites 677 and 678 and those that are found remain fresh and glassy (Schmincke, 1983, Leg 111 Scientific Party, 1988). The clay and silt fractions which contain illite, kaolinite and quartz of main continental origin are restricted to the continental margin and to the neighbouring deepest part of the Panama Basin approximately at 3,000-3,400m depths (Van Andel, 1973, Heath *et al.*, 1974). Thus it seems likely that the aluminous smectite originated from land and was subsequently transported and deposited at Sites 677 and 678 without change of its chemical composition.

The chemical composition of Fe-rich smectite from Sites 677 and 678 averages 55.8% SiO_2, 13.9% Al_2O_3, 6.5% MgO, 3.9% CaO, 17.1% Fe_2O_3*, 1.7% K_2O, and 1.2% Na_2O. The calculated formula is $Si_{3.58}Al_{1.05}Mg_{0.61}Ca_{0.27}Fe_{0.83}K_{0.14}Na_{0.15}$ while the formula of Mg-rich smectite is $Si_{3.25}Al_{1.07}Mg_{0.86}Ca_{0.75}Fe_{0.68}K_{0.20}Na_{0.31}$. The cation abundances in Table 4 were calculated by adjusting the formula so that the totals for the octahedral layer and the interlayer-layer charges were closest to "ideal values", i.e., an octahedral total of 2.00 and balanced interlayer-layer charge. The resulting structural formula indicates that both iron-rich and magnesium-rich smectites belong to the same series of solid solution. Our results are in better agreement with those of Aoki *et al.* (1974, 1978) and Hein *et al.* (1979) than those of Corliss *et al.* (1978) or Dymond and Eklund (1978) who have described the smectite phase in their samples to be nontronite. Aoki *et al.* (1974) proposed that iron-rich smectite is of hydrothermal origin. Bischoff and Rosenbauer (1977) considered them to have formed by reaction between hydrothermal solution and seawater. Fe-rich smectites from Hole 677 A would have formed under these conditions.

4. 3 Hydrothermal activity in the flank province of the Costa Rica Rift

Accumulation Rate of Al, Mn, Cu, Zn and $CaCO_3$

The abundance of Fe-rich smectite, the high heavy metal content of the fine size fraction, and the negative Ce anomaly indicate that hydrothermal components have contributed sediments from Sites 677 and 678. Because Site 677 was located at the spreading center of the Costa Rica Rift about 6.2 million years ago and has subsequently moved to the flank province, the accumulation rates of elements by hydrothermal activity can be traced.

The flux of each element can be calculated from the sedimentation rate, density of sediments and the concentration of the element. The results are shown in Table 8 and Fig. 6. The accumulation rate of $CaCO_3$ was large, 3-7 $g/cm^2 10^3$year from 6.2 Ma to 4.3 Ma, decreased abruptly then the gradually to 0.2 $g/cm^2 10^3$ year at the present. The possible reasons for this trend are that (1) the basement of Site 677 subsided, (2) the calcite compensation depth fluctuated, (3) the geographic locations changed and (4) surface-water productivity changed (Beiersdorf *et al.*, 1983). Al is an important element of nonbiogenic fractions such as detri-

Table 8 Accumulation rate of elements in sediments from Hole 677A.

Core	1	6	12	18	23	27	31
Section	3	6	4	3	4	4	4
Interval (cm)	148	123	123	123	148	148	123
Depth (m)	4.5	48.4	106.9	158.0	208.1	246.8	285.0
Sedimentation rate (m/million years)							
	33.3	45.5	57.7	63.3	120.9	83.4	101.2
Porosity (%)	85.65	77.25	81.44	80.65	65.97	81.28	73.67
Density (g/cc)*	2.25	1.71	3.44	3.29	2.17	2.91	3.07
mg/cm 1000 yr							
SiO_2	544	558	1465	1097	1249	1034	1611
TiO_2	3	5	10	7	4	2	4
Al_2O_3	106	121	256	203	95	35	92
Fe_2O_3*	34	55	138	95	62	27	67
MnO	2	5	12	10	14	5	11
MgO	18	33	82	83	57	23	52
CaO	139	478	758	1266	4042	1860	3501
Na_2O	27	22	59	32	0	5	0
K_2O	24	8	38	11	1	2	2
P_2O_5	1	2	6	8	12	5	16
S	9	9	9	20	25	13	23
$CaCO_3$	228	804	1347	2260	7054	3274	5758
μg/cm 1000 yr							
Co	12	23	94	37	30	8	66
Cr	66	135	257	89	135	36	53
Ni	166	267	727	450	609	237	441
Li	42	54	123	68	107	22	15
Nb	3	4	4	10	0	0	5
Zr	72	92	199	165	125	18	115
Y	19	35	88	81	80	27	98
Sr	513	1434	2643	3742	9520	3221	8286
Rb	57	39	88	73	45	9	41
	0	0	0	0	0	0	0
Mn	1832	4110	9117	7802	11049	4214	8230
Cu	118	145	399	465	408	197	409
Zn	268	379	862	692	895	418	642
Heavy Metal Flux by Hydrothermal Activity							
μg/cm 1000 yr							
Mn	581	1912	4933	5121	6246	—	4662
Cu	48	11	44	78	63	—	29
Zn	64	94	366	259	312	—	121

Note : Density=Grain density (g/cc)

tal materials and clay minerals. The Al_2O_3 accumulation rate was low, about 100 mg/cm^2 10^3year from 6.2 Ma to 4.3 Ma, increased from 4.3 Ma to 2.2 Ma, and has been relatively constant during the last 2 million years.

The amounts of Mn, Cu and Zn extracted with hydroxylamine hydrochloride-acetic acid are considered to correspond to those present

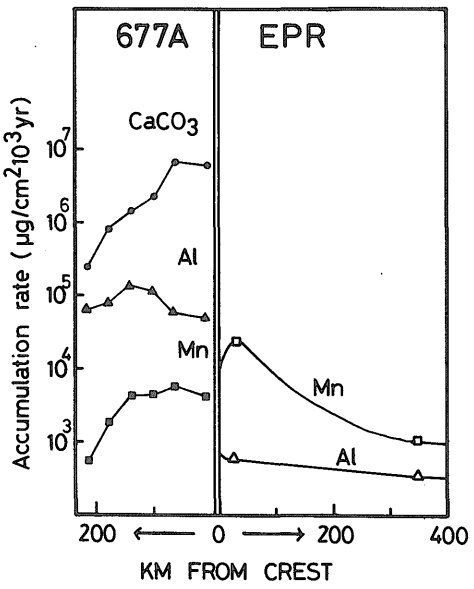

Fig. 6 Acccumulation rates of $CaCO_3$, Al and hydrothermal Mn versus distance from the crest of Hole 677 A in comparison with those estimated from East Pacific Rise by Dymond *et al.* (1975).

as oxide and/or hydroxide because the metal content of original foraminifer tests is negligible (a few ppm). The accumulation rates of hydrothermal Mn, Cu and Zn from 6.2 Ma to 2.2 Ma were 4.7–6.2 mg/cm^{2}10^{3}yr, 29–78μg/cm^{2}10^{3}yr and 121–366μg/cm^{2}10^{3}yr, respectively. They have decreased since 2.2 Ma to 0.6–1.9 mg/cm^{2}10^{3}yr, 11–48μg/cm^{2}10^{3}yr and 64–94μg/cm^{2}10^{3}yr, respectively.

Bender and Broecker (1970) have determined the manganese accumulation rates in 38 pelagic sediments. They range from 0.2 to 3.2 mgMn/cm^{2}10^{3}yr with an average value 1.3 mg/cm^{2}10^{3}yr. The manganese accumulation rate is 35 mg/cm^{2}10^{3}yr on 1 Ma crust at 17°S East Pacific Rise (EPR) and falls off rapidly to 1.7 mg/cm^{2}10^{3}yr at about 3.5 Ma on the western flank of the EPR (Bender *et al.*, 1971). The manganese accumulation rate is 5.8 mg/cm^{2}10^{3}yr at 11°S EPR (Dymond and Veeh, 1975). Mn accumulation rates for Hole 677A are higher than those for previous observed pelagic sediments and are comparable to those near the spreading axis of the EPR (Fig. 6).

Origin of hydrothermal components in sediments from Hole 677A

The constant, high accumulation rates of heavy metals continued from 6.2 Ma to 2.2 Ma in Hole 677A, unlike that found on the EPR. Possible reasons for this relation between accumulation rate and age are that (1) productivity of suspended matter near the spreading axis changed, (2) the geographic location changed, (3) bottom water circulation changed or (4) there was a contribution from off-axis hydrothermal activity.

Intense hydrothermal activity is generaly related to spreading rate because the production of high-temperature hydrothermal solution requires much heat energy from magma and hot rocks. Based upon the pattern of magnetic anomalies, the spreading rate of the Costa Rica Rift has been relatively constant during the last 6 million years. Also, a large geographic change in the Panama Basin is not supported by tectonic and sedimentological evidence (Lonsdale and Klitgord, 1978; Beiersdorf and Natland, 1983). The western Panama Basin is bordered by the Cocos Ridge (to the west and north), the Carnegie Ridge (to the south), the Malpelo Ridge (to the east) and the Coiba Ridge (to the east). Bottom water from the Peru Basin flows to the Panama Basin through the saddle between the Malpelo and Carnegie Ridges and spreads out (Lonsdale, 1977). The similar basic structure of the basins between 6.2 Ma and the present precludes a very different bottom water circulation at about 6.2 Ma.

Suspended particles from active hydrothermal vents are condensed above and near vent fields (McConachy and Scott, 1987) and at the Mid-Atlantic Ridge, particulate Zn and Cu values decrease dramatically away from the vent source (Trocine and Trefry 1988). If hydrothermal suspended matter comes only from hydrothermal activity along the spreading axis and its production rate is relatively constant, the flux of heavy metals to the sediments should decrease as an increase of the distance from the axis. Rapid decreases of accumulation rate of Mn and Al/(Al+Fe+Mn) ratio are found adjacent to EPR and Mid-Atlantic Ridge

(Bostom and Peterson, 1969 ; Bostom, 1975).

A single source of hydrothermal suspended matter cannot explain such a constant and high value of accumulation rates for Hole 677A. The heat flow oscillates between high and low values in a systematic matter at progressively greater distances from the crest of the Galapagos Spreading Center (Williams *et al.*, 1974). The observed conductive heat flux rarely exceeded the theoretical or expected value for that age, while the observed mean heat flow was much lower than expected. All these observations are characteristic of convective heat transfer.

Rows of hydrothermally deposited mounds are located in a band of sea floor with high heat flow from 18 to 25km south of the rift axis in crust from 0.5 Ma to 0.7 Ma. This high heat flow zone is interpreted to be a limb of a hydrothermal convective cell (Corliss *et al.*, 1978 ; Corliss *et al.*, 1979). When a thick, uniform blanket of sediment covers all basement relief, the mean observed heat flow approaches the theoretical value predicted for the age of that particular segment of sea floor. In general, more than 200 m thick sediments prevents hot circulating solution from pouring out of seafloor. About 200 m of calcareous ooze deposited over the oceanic crust around Sites 677 and 678 about 2 Ma, when the heat flow appears to have increased to values similar to those predicted by plate models (Anderson and Skilbeck, 1981). The event is consistent with the decrease in the heavy metal accumulation rate in Hole 677A. Flank hydrothermal activity would appear to account for the heavy metal accumulation rate in Hole 677A.

5. Acknowledgement

The authors wish to acknowledge Dr. Gorton, M. for providing technical advice on the analytical procedure and a reviewer to give us comments to improve this paper. This work was supported by Research grant of the Agency of Industrial Science and Technology to H.K. and NSERC Grant to S.D.S..

References

Alt, J.C., Honnorez, J., Laverne, C. and Emmermann, R. (1986) Alteration of a 1km section through the upper oceanic crust, DSDP Hole 504B : The mineralogy, chemistry and evolution of basalt-seawater interactions. *J. Geophys. Res.*, vol. 91, p. 10309–10335.

Anderson, R.N., Honnorez, J., Becker, K., Adamson, A.C., Alt, J.C., Emmermann, R., Kempton, P.D., Kinoshita, H., Laverne, C., Mottl, M.J. and Newmark, R.L. (1982) DSDP Hole 504B, the first reference section over 1 km through Layer 2 of the oceanic crust. *Nature*, vol.300, p.589–594.

——— and Skilbeck, J.N. (1981) Oceanic heat flow. Emiliani, C. ed., *The Sea*, Wiley, vol. 7, p.489–524.

Aoki, S., Oinuma, K. and Sudo, T. (1974) An iron-rich montmorillonite in a sediment core from the northeastern Pacific. *Deep-Sea Res.*, vol. 21, p. 865–875.

———, Kohyama, N. and Sudo, T. (1979) Mineralogical and chemical properties of smectites in a sediment core from the southeastern Pacific. *Deep-Sea Res.*, vol. 26 A, p. 893–902.

Beiersdorf, H. and Rosch, H. (1983) Mineralogy of sediments encountered during Deep Sea Drilling Project Leg 69 (Costa Rica Rift, Panama Basin), as determined by X-ray diffraction. *In* Cann, J.R., Langseth, M.G. *et al., Init. Repts. DSDP,* vol. 69 : Washington (U.S. Govt. Printing Office), p. 385–393.

——— and Natland, J.H. (1983) Sedimentary and diagenetic processes in the Central Panama Basin since the late Miocene : The lithology and composition of sediments from Deep Sea Drilling Project Sites 504 and 505. *In* Cann, J.R., Langseth, M.G. *et al., Init. Repts. DSDP,* vol. 69 : Washington (U.S. Govt. Printing Office), p. 343–383.

Bender, M., Broecker, W.S. Gornitz, V., Midel, U., Kay, R., Sun, S.-S., and

Biscaye, P. (1971) Geochemistry of three cores from the East Pacific Rise. *Earth Planet. Sci. Lett.,* vol. 12, p. 425–433.

Bender, M., Ku, T.-L. and Broecker, W.S. (1970) Accumulation rates of manganese in pelagic sediments and nodules. *Earth Planet. Sci. Lett.,* vol. 8, p. 143–148.

Bischoff, J.L. and Rosenbauer, R.J (1977) Recent metalliferous sediments in the north Pacific manganese nodule area. *Earth Planet. Sci. Lett.*, vol. 33, p. 379–388.

Bolger, G.W., Betzer, P.R. and Gordeev, V.V. (1978) Hydrothermally-derived manganese suspended over the Galapagos Spreading Center. *Deep-Sea Res.* a, vol. 25, p. 721–733.

Boström, K. and Peterson, N.A. (1969) The origin of aluminum-poor ferromanganoan sediments in areas of high heat flow on the East Pacific Rise. *Marine Geology,* vol. 7, p.427–447.

——— (1975) The origin and fate of ferromanganoan active ridge sediments. *Stockholm Contrib. Geol.*, vol. 27, p. 149–243.

Boyle, E.A. (1981) Cadmium, zinc, copper and barium in foraminifera tests. *Earth Planet. Sci. Lett.*, vol.53, p.11–35.

Chester, R. and Hughes, M.J. (1967) A chemical technique for the separation of ferro-manganese minerals, carbonate minerals and adsorber trace elements from pelagic sediments. *Chem. Geol.*, vol. 2, p. 249–262.

Corliss, J.B., Dymond, J., Gordon, L.I., Edmond, J.M., von Herzen, R.P., Ballard, R.D., Green, H., Williams, D., Bainbridge, A., Crane, K. and van Andel, T.H. (1979) Submarine thermal springs on the Galapagos Rift. *Science*, vol.203, p. 1073–1083.

———, Lyle, M., Dymond, J. and Crane, K. (1978) The chemistry of hydrothermal mounds near the Galapagos Rift. *Earth Planet. Sci. Lett.*, vol. 40, p. 12–24.

Dymond, J., Corliss, G.R., Heath, C.W., Field, E.J. Dasch and Veeh, H.H. (1973) Origin of metallifeour sediments from the Pacific Ocean. *Geol. Soc. Amer. Bull.*, vol. 84, p. 3355–3372.

——— and Eklund, W. (1978) A microprobe study of metalliferous sediment components. *Earth Planet. Sci. Lett.,* vol. 40, p. 243–251.

——— and Veeh, H.H. (1975) Metal accumulation rate in the Southeast Pacific and the origin of metallieferous sediments. *Earth Planet. Sci. Lett.,* vol. 28, p. 13–22.

Edmond, J.M., McDuff, R.E., Chan, L.H., Collier, R., Grant, B., Gordon, L.I. and Corliss, J.B. (1979) Ridge crest hydrothermal activity and the balances of the major and minor elements in the ocean : the Galapagos data. *Earth Planet. Sci. Lett.,* vol. 46, p. 1–18.

Goldberg, E.D. and Arrhnenius, G.O.S. (1958) Chemistry of Pacific pelagic sediments. *Geochim. Cosmochim. Acta,* vol. 13, p. 153–212.

Hein, J.R., Yeh, H.W. and Alexander, E.R. (1979) Origin of iron-rich montmorillonite from the manganese nodule belt of the North Equatorial Pacific. *Clay Clay Miner.*, vol. 27, p. 185–194.

Heath, G.R., Moore, JR, T.C. and Roberts, G.L. (1974) Mineralogy of surface sediments from the Panama Basin, Eastern Equatorial Pacific. *J. Geology,* vol. 82, p. 145–160.

Kawahata, H. and Furuta, T. (1985) Subsea-floor hydrothermal alteration in the Galapagos Spreading Center. *Chem. Geol.,* vol. 49, p. 259–274.

———, Kusakabe, M. and Kikuchi, Y. (1987) Strontium, oxygen and hydrogen isotope geochemistry of hydrothermally altered and weathered rocks in DSDP Hole 504B, Costa Rica Rift. *Earth Planet. Sci. Lett.,* vol. 85, p. 343–355.

Kowsmann, R.O. (1973) Coarse components in surface sediments of the Panama Basin, Eastern Equatorial Pacific. *J. Geology,* vol. 81, p. 473–494.

Langseth, M.G., Mottl, M.J., Hobart, M.A. and Fisher, A. (1988) The distribution of geothermal and geochemical gradients near Site 501/504 : imlica-

tions for hydrothermal circulation in the oceanic crust. *In* Becker, K., Sakai, H. *et al., Proc. ODP, Init. Repts.* (*Pt. A*), vol. 111 : Washington (U.S. Govt. Printing Office), p.23-34.

Leg 111 Shipboard Scientific Party (1987) News from a deepening hole. *Nature,* vol. 325, p. 484-485.

——— (1988) Site Reports. Sites 677 and 678. *In* Becker, K., Sakai, H. *et al., Proc. ODP, Init. Repts.* (*Pt. A*), vol. 111 : Washington (U.S. Govt. Printing Office), p. 253-348.

Lonsdale, P. (1977) Inflow of bottom water to the Panama Basin. *Deep-Sea Res.,* vol. 24, p. 1065-1101.

Leg 111 Shipboard Scientific party and Klitgord, K.D. (1978) Structure and tectonic history of the eastern Panama Basin. *Geol. Soc. Amer. Bull.*, vol. 89, p. 981-999.

McConachy, T.F. and Scott, S.D. (1987) Real-time mapping of hydrothermal plumes over Southern Explorer Ridge, NE Pacific Ocean. *Marine Mining*, vol. 6, p. 181-204.

Moore, JR, T.C., Heath, G.R. and Kowsmann, R.O. (1973) Biogenic sediments of the Panama Basin. *J. Geology*, vol.81, p. 458-472.

Mottl, M.J., Lawrence, J.R. and Keigwin, L.D. (1983) Elemental and stable-isotope composition of pore waters and carbonate sediments from Deep Sea Drilling Project Sites 501/504 and 505. *In* Cann, J.R., Langseth, M.G. *et al., Init. Repts. DSDP,* vol. 69 : Washington (U.S. Govt. Printing Office), p. 461-473.

Piper, D.Z. (1974) Rare earth elements in sedimentary cycle : a summary. *Chem. Geol.*, vol. 14, p. 285-304.

Schmincke, H.U. (1983) Rhyolitic and basaltic ashes from the Galapagos mounds area, Leg 70, Deep Sea Drilling Project. *In* Cann, J.R., Langseth, M.G. *et al., Init. Repts. DSDP,* vol. 69, Washington (U.S. Govt. Printing Office), p. 451-457.

Trocine, R.P. and Trefry, J.H. (1988) Distribution and chemistry of suspended particles from an active hydrothermal vent site on the Mid-Atlantic Ridge at 26 oN. *Earth Planet. Sci. Lett.,* vol.88, p.1-15.

Van Andel, T.H. (1973) Texture and dispersal of sediments in the Panama Basin. *J. Geology,* vol. 81, p. 434-457.

Von Damm, K.L., Edmond, J.M., Grant, B,, Measures, C.I., Walden, B. and Weiss, R.F. (1985) Chemistry of submarine hydrothermal solutions at 21°N, East Pacific Rise. *Geochim. Cosmochim. Acta,* vol. 49, p. 2197-2220.

Williams, D.A., Von Herzen, R.P., Sclater, J.G. and Anderson, R.N. (1974) The Galapagos Spreading Center : lithospheric cooling and hydrothermal circulation. *Geophys. J. Roy. Ast. Soc.*, vol. 38, p. 587-608.

Bulletin of the Geological Survey of Japan, Vol. 42, No. 4

パナマ海盆コスタリカ・リフトにおける堆積物の地球化学

川幡穂高・青木三郎・S.D. スコット・石塚明男

要　旨

ODP 677, 678 掘削点は，パナマ海盆の高生物生産域に位置している．堆積物のサンドとシルトサイズは主に生物遺骸や陸源砕屑物から，クレイサイズは粘土鉱物や生物遺骸の破片から構成されている．アルミニウム（Al）スメクタイトは，陸源性であるが，鉄（Fe）スメクタイトは熱水起源である．

堆積物中のマンガン（Mn），銅（Cu），亜鉛（Zn）含有量は，多量の生物遺骸の寄与による希釈効果によって，低い濃度を示しているが，セリウムの負の異常，重金属/アルミニウム比と希土類元素/アルミニウム比のよい相関からこれらの重金属の一部は熱水起源物質に取り込まれていることが示される．特に，塩酸ヒロドオキシルアミン-酢酸によって抽出されたマンガン，銅，亜鉛は熱水活動に関係したものと考えられる．これらの元素の集積速度は，それぞれ，620 万年から 220 万年前の間は 4.7-6.2 $mg/cm^2\ 10^3\ yr$，29-78 $\mu g/cm^2\ 10^3\ yr$，121-366 $\mu g/cm^2\ 10^3\ yr$，220 万年前から現在までは，減少し，0.6-1.9 $mg/cm^2\ 10^3\ yr$，11-48 $\mu g/cm^3\ 10^3\ yr$，64-94 $\mu g/cm^2\ 10^3\ yr$ である．677 A 掘削孔の熱水性マンガンの集積速度は，遠洋性堆積物で通常観察される値よりやや大きく，東太平洋海膨の拡大軸付近で観察される値に匹敵する．このような高い値が約 400 万年続いたのは，たぶんリフト裾野での熱水活動の寄与があったためと考えられる．

（受付：1991 年 1 月 21 日；受理：1991 年 2 月 7 日）